The Effect of Temperature on Product Distribution over Fe-Cu-K Catalyst in Fischer-Tropsch Synthesis

Yahya Zamani[1], Ali Mohajeri[1]*, Mehdi Bakavoli[2], Mohamad Rahimizadeh[2], and Seyed Mohamad Seyedi[2]

[1]Gas Division, Research Institute of Petroleum Industry (RIPI), Tehran, Iran
[2]Department of Chemistry, Ferdowsi University of Mashhad, Mashhad, Iran

ABSTRACT

The iron-based catalyst was prepared by a microemulsion method. The composition of the final nanosized iron catalyst, in terms of the atomic ratio, contains 100Fe/4Cu/2K. The experimental techniques of XRD, BET, TEM, and TPR were used to study the phase, structure, and morphology of the catalyst. Fischer-Tropsch synthesis (FTS) reaction test was performed in a fixed bed reactor under pressure of 17 bar, temperature of 270-310 °C, H_2 to CO ratio of 1, and a Gas Hourly Space Velocity (GHSV) of 3 $nl.hr^{-1}.gCat^{-1}$. The temperature of the system as a key parameter was changed and its effect on the selectivity and reaction rate was analyzed. The results show that the rates of both reactions including FTS and water-gas shift (WGS) raised by increasing temperature. For this condition, CO conversion was also increased up to 87.6%.

Keywords: Nanoparticles, Iron Catalyst, Catalyst Characterization, Fischer-Tropsch Synthesis

INTRODUCTION

Presently, crude oil is the main source of liquid fuels and chemicals, but its reserve is in exhaustion. At the same time, the environment is damaged by the pollutants from the consumption of fuels. New technologies, which can supply environmental-friendly fuels, are required to overcome the above problems. Fischer–Tropsch synthesis is one of the methods to meet the demand for the clean transportation of fuels (gasoline and diesel) and chemicals (in particular α-olefins) [1-5]. FT synthesis has successfully been commercialized to produce fuel from coal and natural gas [6-9]. Because the reserves of coal and natural gas are richer than those of crude oil [2,9-11], FT synthesis can supply plentiful liquid fuels for the world in longer times than petroleum refining. The most common Fischer–Tropsch catalysts are group VIII metals (Co, Ru, and Fe). Nanoparticles may offer different morphology and increase surface area, which, in theory, should enhance the reaction rates as a result of more available catalyst sites. Therefore, for exothermic reactions such as CO hydrogenations, nanocatalysts are supposed to be more effective and selective. Iron catalysts are commonly used because of their low costs in comparison to other active metals. Alkali-promoted iron catalysts have industrially been applied to the Fischer–Tropsch synthesis for many years [12-15]. These catalysts have a high water-gas shift activity and high selectivity for olefins and appear to be stable, when synthesis gas at a high H_2 to CO ratio is converted

***Corresponding author**
Ali Mohajeri
Email: mohajeria@ripi.ir
Tel: +98 21 4825 2090
Fax: +98 21 44739716

Article history
Received: January 11, 2015
Received in revised form: December 02, 2015
Accepted: February 04, 2016
Available online: January 23, 2016

[16, 17]. Iron catalysts are often promoted with Cu, which increases the rate of reduction, enabling a lower reduction temperature [18-20]. According to Anderson [20] the distribution for n-paraffins can be described by the Anderson–Schulz–Flory (ASF) equation (Equation 1):

$$m_n = (1-\alpha)\alpha^{n-1} \quad (1)$$

where, the growth probability factor α is independent of n. m_n is the mole fraction of a hydrocarbon with a chain length of n.

The process conditions, as well as the catalyst characteristics, influence the product selectivity [21, 22]. Although extensive research has been carried out on the effect of potassium promoter on the structure of iron catalyst [23], the study of operating conditions, including temperature as an important variable is scarce. An increase in reaction temperature results in a shift toward products with a lower carbon number on iron [24], ruthenium [25], and cobalt catalysts [25]. Donnelly and Satterfield [24] and Anderson [20] observed an increase in the olefin to paraffin ratio with increasing temperature on potassium-promoted precipitated iron catalysts. However, Dictor and Bell [26] reported a decrease in the olefin selectivity by increasing temperature for unalkalized iron oxide powders. One of the parameters affecting product selectivity and catalyst activity is the reaction temperature. If the temperature is raised above an optimum limit, the catalyst deactivation and coke formation will happen. In this work, the activity of Fe-Cu-K catalyst over the temperature range of 270 to 310 °C is considered to determine the optimum reaction temperature.

EXPERIMENTAL PROCEDURES

Catalyst Preparation

Nanostructured iron catalysts were prepared by a microemulsion method. A water solution of metal precursors ($FeCl_3.6H_2O$) was added to a mixture of 2-propanol and chloroform and sodium dodecyl sulfate (SDS) as a surfactant. Hydrazine (25-30%), in the aqueous phase, was added as a precipitating agent and stirred for 4 hrs. The solid was recovered by centrifugation and washed thoroughly with distilled water, ethanol, and acetone. Finally, the samples were dried overnight at 110 °C, and subsequently calcined in air at 380 °C for 4 hrs. Nanostructured potassium and copper oxides were prepared like nanostructured Fe and they were then mixed together. The promoted catalysts were dried at 110 °C for 15 hrs and calcined at 380 °C for 4 hrs in air [27,28]. The catalyst was pressed into pellets, crushed, and sieved to obtain particles with a mesh of 30-40.

Catalyst Characterization

The BET surface area and pore volume of the catalysts were determined by N_2 physisorption using a Micromeritics ASAP 3020 automated system. A 0.3 gr catalyst sample was degassed in the system at 100 °C for 1 hr and then at 300 °C for 2 hrs prior to analysis. The analysis was done using N_2 adsorption at -196 °C. The average particle size of the calcined powders was measured by LEO 912AB TEM. The XRD spectra of the fresh catalyst were recorded with a Philips PW1840 X-ray diffractometer with monochromatized Cu (Kα) radiation to determine the iron phases. The temperature-programmed reduction (TPR) profiles of the calcined catalysts were recorded using a Micromeritics TPD-TPR 290 system. The TPR of 50 mg of each sample was performed in a gas mixture consisting of 5% H_2 and 95% argon. The sample was heated from 50 to 900 °C at a heating rate of 10 °C/min. The H_2 reduction process illustrated three stages in the temperature range of 200-900 °C.

Reactor System and Operating Procedure

As shown in Figure 1, the catalytic reaction experiments were conducted in a fixed bed stainless steel reactor. The flow rate of inlet gases and reactor pressure were controlled by electronic mass flow and pressure controllers respectively. A four heating zone furnace

equipped with a temperature controller and an indicator supplied the required reaction heat.

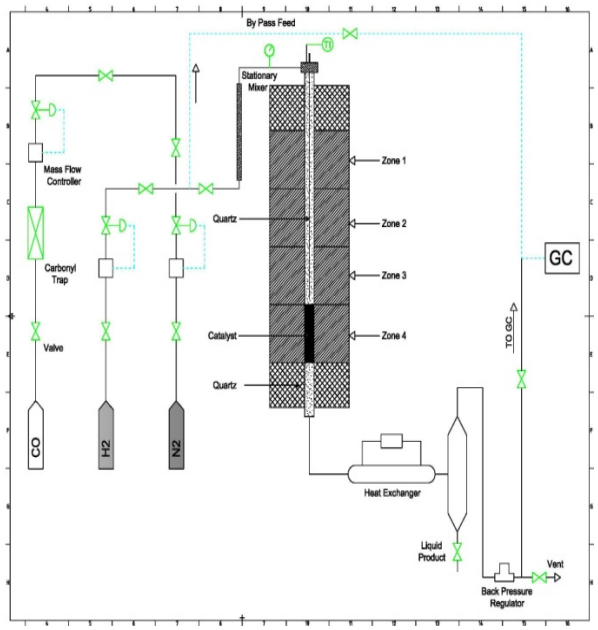

Figure 1: Catalyst test system.

The reactor was loaded by 1 gr of catalyst. The catalyst was reduced under a 10% H_2/N_2 flow for 3 hrs. The catalyst activation was followed in a stream of synthesis gas at an H_2 to CO ratio of 1 and an SV of 1.5 $nl.hr^{-1}.gCat^{-1}$ for 24 hrs at atmospheric pressure and a temperature of 270 °C. Following the activation process, the reactor pressure was raised to 17 bar and the reaction temperature was increased to 270-310 °C. The reaction initiated in synthesis gas stream at an H_2 to CO ratio of 1 and a GHSV of 3 $nl.hr^{-1}.gCat^{-1}$.

Product Analysis

The products were analyzed by two gas chromatographs (Varian CP 3800). The first one includes two packed columns connected to two thermal conductivity detectors (TCD), which were used for analyzing H_2, CO, CO_2, CH_4, and other non-condensable gases. The other one with a Petrocol Tm DH100 fused silica capillary column was attached to a flame ionization detector (FID) for analyzing organic liquid products [29, 30]. The activities and product selectivity were assessed after 72 hrs.

RESULTS AND DISCUSSION

Alkaline elements are used as promoters, because they can modify the adsorption pattern of the reactants (H_2 and CO) on the active sites. The overall effects of these promoters such as potassium on the behavior of the iron-based FTS catalysts, namely CO chemisorptions enhancement, has been justified as a consequence of the iron tendency to withdraw electronic density from potassium. Therefore, the strength of the Fe-CO bond was enhanced. Table 1 shows the BET results for the catalyst surface area. By adding potassium, the BET surface area and pore volume in the catalyst decreased as potassium promoted the aggregation of the catalyst crystallites and blocked up the pore volume of the catalyst.

Table 1: Catalysts surface area.

Catalysts	BET Surface area(m^2/g)	Pore Volume(cm^3/g)
100Fe/4Cu/2K	45.5	0.24

The X-ray diffraction patterns of the prepared catalyst (Figure 2) show narrow and high intensity peaks, suggesting that the sample should highly be crystalline consisting of small particle sizes and that the most abundant phase should be Fe_2O_3.

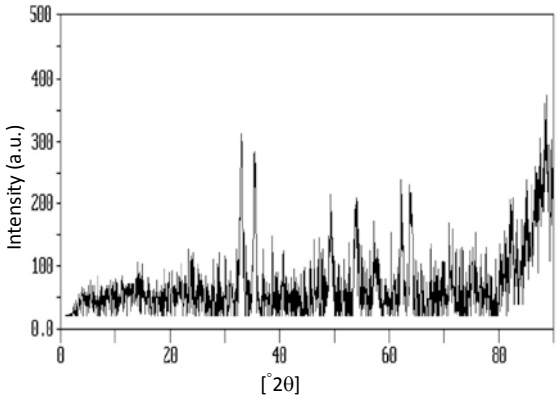

Figure 2: XRD spectra of the fresh 100Fe/4Cu/2K catalyst.

The morphology of the catalysts was analyzed by TEM images as shown in Figure 3. Although TEM revealed that the diameter of the nanoparticle was in the range of 10 to 40 nm, the difference

between the catalysts with a diverse ratio of metal oxides was obscure.

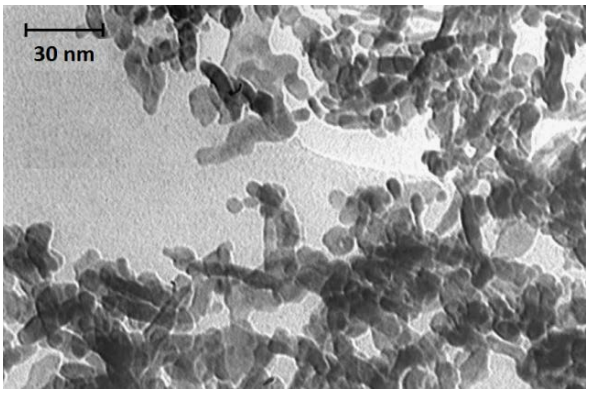

Figure 3: TEM micrograph of 100Fe/4Cu/2K catalyst.

Figure 4 shows the H_2-TPR profiles of the nanosized iron catalyst; this curve determines the reduction behavior of the catalyst. The first stage is ascribed to the transformations of CuO to Cu; the second stage is attributed to the transformation of Fe_2O_3 to Fe_3O_4; the third stage represents the transformation of Fe_3O_4 to Fe [31].

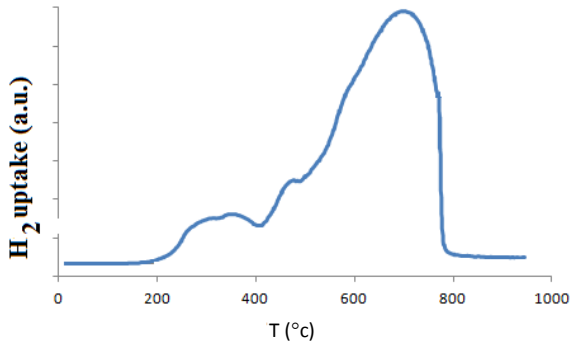

Figure 4: H_2-TPR profiles of the catalyst.

Figure 5 shows the rates of FTS and WGS at different temperatures.

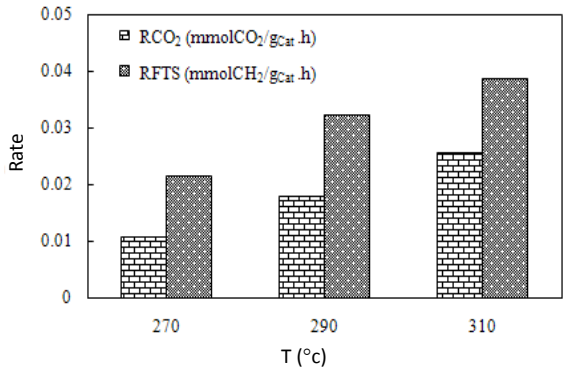

Figure 5: Rates of FTS and WGS.

Figure 6 shows CO conversion and chain growth probability at different temperatures. It can be seen that with increasing temperature from 270 to 310 °C, the CO conversion gradually increased from 63.3% to 87.6%. It seems that the increasing temperature has a significant influence on CO_2 selectivity, which increases from 25.3% to 42.7% in the temperature range of 270 to 310 °C. In fact, the increase in temperature enhances the catalyst activity.

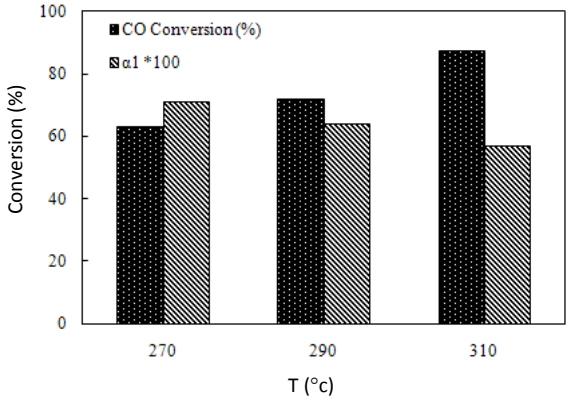

Figure 6: Effect of temperature on CO conversion and chain growth probability.

Figure 7 shows the product selectivity of the catalyst at different temperatures. According to this figure, the selectivity of light hydrocarbons including methane and C_2 to C_4 is improved by increasing the temperature of the system.

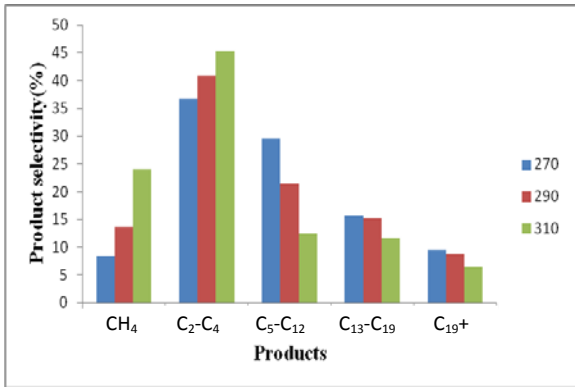

Figure 7: Product selectivity of the catalyst at different temperatures (time of reaction: 72 hrs, *P*= 1.7 MPa, $H_2/CO = 1$, and SV= 3 nl.gCat.$^{-1}$hr^{-1}).

On the other hand, the selectivity of higher hydrocarbons decreases by increasing temperature; it should be noted that selectivity to oxygenates

was negligible (<3%) in all the cases. All the results imply that the rate of hydrogenation reactions is enhanced, when temperature rises.

Figure 8 shows the olefin to paraffin ratio of the catalyst at different temperatures. This figure shows that the olefin to paraffin ratio of the catalyst is enhanced when temperature rises. However, the reaction conditions influence the product selectivity.

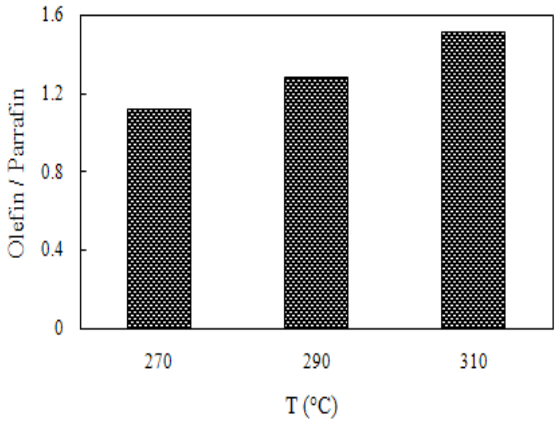

Figure 8: Olefin to paraffin ratio of the catalyst at different temperatures.

CONCLUSIONS

Nanostructured iron catalysts were prepared by the microemulsion method. Potassium-promoted iron nanocatalysts were studied using different characterization techniques. The effect of temperature on the Fischer-Tropsch synthesis activity and selectivity was investigated in a fixed bed reactor. It was observed that the activity and methane selectivity increased, while C_5^+ selectivity decreased by increasing temperature. The changes in the catalytic performances can be attributed to the effect of temperature on H_2 adsorption, which significantly affects the FTS performance of the catalysts. The optimum temperature for the reaction condition of the mentioned catalyst is estimated to be 290 °C.

ACKNOWLEDGEMENTS

We are grateful to the Research and Development of National Iranian Oil Company (NIOC) for their financial support.

REFERENCES

[1] Schulz H., "Short History and Present Trends of Fischer–Tropsch Synthesis," *Applied Catalysis A: General*, **1999**, *186*, 3-12.

[2] Dry M. E., "Fischer–Tropsch Reactions and the Environment," *Applied Catalysis A: General*, **1999**, *189*, 185-190.

[3] Rabiu A. M., Steen E. V., and Claeys M., "Further Investigation into the Formation of Alcohol during Fischer Tropsch Synthesis on Fe-based Catalysts," *APCBEE Proc.*, **2012**, *3*, 110-115.

[4] Nakhaei Pour A. and Housaindokht M. R., "The Olefin to Paraffin Ratio as a Function of Catalyst Particle Size in Fischer-Tropsch Synthesis by Iron Catalyst," *Journal of Natural Gas Science and Engineering*, **2013**, *14*, 204-210.

[5] Kang S. H., Koo H. M., Kim A. R., Lee D. H. et al., "Correlation of the Amount of Carbonaceous Species with Catalytic Performance on Iron-based Fischer-Tropsch Catalysts," *Fuel Processing Technoligy*, **2013**, *109*, 141-149.

[6] Sie S. T., Senden M. M. G., and Van Wechem H. M. H., "The Pivotal Role of Catalysis in Energy Related Environmental Technology," *Catalysis Today*, **1999**, *8*, 371-380.

[7] Espinoza R. L., Steynberg A. P., Jager B., and Vosloo A. C., "Low Temperature Fischer-Tropsch Synthesis from a Sasol Perspective," *Applied Catalysis A: General*, **1999**, *186*, 13-26.

[8] Steynberg A. P., Espinoza R. L., Jager B., and Vosloo A. C., "High Temperature Fischer-Tropsch Synthesis in Commercial Practice," *Applied Catalysis A: General*, **1999**, *186*, 41-54.

[9] Dry M. E., "The Fischer-Tropsch Process: 1950-2000," *Catalysis Today*, **2002**, *71*, 227-241.

[10] Schobert H. H. and Song C., "Chemicals

and Materials from Coal in the 21st Century," *Fuel*, **2002**, *81*, 15-32.

[11] Alpern B. and Lemos de Sousa M. J., "Documented International Enquiry on Solid Sedimentary Fossil Fuels; Coal: Definitions, Classifications, Reserves-resources, and Energy Potential," *International Journal of Coal Geology*, **2002**, *50*, 3-41.

[12] Van Der Laan G. P. and Beenackers A. A. C. M. "Kinetics and Selectivity of the Fischer-Tropsch Synthesis: A Literature Review," *Catalysis Reviews*, **1999**, *41*, 255-318.

[13] Rao V. U. S., Stiegel G. J., Cinquegrane G. J., and Srivastave R. D., "Iron-based Catalysts for Slurry-phase Fischer-Tropsch Process: Technology Review," *Fuel Processing Technology*, **1992**, *30*, 83-107.

[14] Nakhaei Pour A., Riyahi F., Housaindokht M. R., Irani M. et al., "Hydrocarbon Production Rates in Fischer-Tropsch Synthesis over a Fe/Cu/La/Si Catalyst," *Journal of Energy Chemical*, **2013**, *22*, 119-129.

[15] Feyzi M. and Jafari F., "Study on Iron-manganese Catalysts for Fischer-Tropsch Synthesis," *Journal of Fuel Chemical Technology*, **2012**, *40*, 550-557.

[16] Jager B. and Espinoza R., "Advances in Low Temperature Fischer–Tropsch," *Catalysis Today*, **1995**, *23*, 17-28.

[17] Kolbel H. and Ralek M., "Fischer-Tropsch Synthesis in the Liquid Phase," *Catalysis Review Science and Engineering*, **1980**, *21*, 225-274.

[18] Roper M., "Fischer Tropsch synthesis," In Catalysis in C_1 Chemistry (W. Keim, ed.), Reidel, Dordrecht, The Netherlands, **1983**, 41–88.

[19] Dry M. E., in Catalysis-Science and Technology (J. R. Anderson and **M. B**oudart eds.), Springer-Verlag, New York, **1981**, 160-255.

[20] Anderson R. B., "Catalysts for the Fischer-Tropsch Synthesis," Van Nostrand Reinhold, New York, **1956**.

[21] Mao W. Y., Sun Q. W., Ying W. Y., and Fang D. Y., "Mechanism of Oxygenates Formation in High Temperature Fischer-Tropsch Synthesis over the Precipitated Iron-based Catalysts," *Journal of Fuel Chemical Technology*, **2013**, *41*, 314-321.

[22] Cano L. A., Cagnoli M. V., Bengoa J. F., Alvarez A. M., et al., "Effect of the Activation Atmosphere on the Activity of Fe Catalysts Supported on SBA-15 in the Fischer–Tropsch Synthesis," *Journal of Catalysis*, **2011**, *278*, 310-320.

[23] Mingsheng L. and Davis B. H. "Fischer-Tropsch Synthesis: Effect of Activation on Potassium Promoted Iron Catalysts," *Fuel Chemistry Division Preprints*, **2002**, *47*, 160-163.

[24] Donnelly T. J. and Satterfield C. N., "Product Distributions of the Fischer-Tropsch Synthesis on Precipitated Iron Catalysts," *Applied Catalysis A: General*, **1989**, *52*, 93-114.

[25] Dry M. E., in Catalysis-Science and Technology (Anderson J. R. and Boudart M., eds.), Springer-Verlag, New York, **1981**, 160-255.

[26] Dictor R. A. and Bell A. T., "Fischer Tropsch Synthesis over Reduced and Unreduced Iron Oxide Catalysts," *Journal of Catalysis*, **1986**, *97*, 121-136.

[27] Nakhaei Pour A., Taghipoor S., Shekarriz M., Shahri S. M. K. et al., "Fisher-Tropsch Synthesis With Fe/Cu/La/SiO_2 Nanostructured Catalyst," *Journal of Nanoscience and Nanotechnology,* **2008**, *8*, 1-5.

[28] Zamani Y., Bakavoli M., Rahimizadeh M., Mohajeri A. et al., "Synergetic Effect of La and Ba Promoters on Nanostructured Iron Catalyst in Fischer-Tropsch Synthesis,"

Chinese Journal of Catalysis, **2012**, *33*, 1119-1124.

[29] Zamani Y., Yousefian S. H., Pour A. N., Moshtari B. et al., "A Method for the Regeneration of Used Fe-ZSM5 Catalyst in Fischer–Tropsch Synthesis," *Chemical Engineering Transfer*, **2010**, *21*, 1045-1051.

[30] Pour A. N., Kamali Shahri S. M., Bozorgzadeh H. R., Zamani Y. et al., "Effect of Mg, La, and Ca Promoters on the Structure and Catalytic Behavior of Iron-based Catalysts in Fischer-Tropsch Synthesis," *Applied Catalysis A: General*, **2008**, *348*, 201-208.

[31] Jin Y. and Datye A. K., "Phase Transformations in Iron Fischer–Tropsch Catalysts during Temperature-programmed Reduction," *Journal of Catalysis*, **2000**, *196*, 8-17.